Amyloid imaging in cognitively normal older adults: Comparison between ^{18}F-flutemetamol and ^{11}C-Pittsburgh Compound B

Katarzyna Adamczuk[1,2], Jolien Schaeverbeke[1,2], Natalie Nelissen[1,3], Veerle Neyens[1,2], Mathieu Vandenbulcke[4], Karolien Goffin[5], Johan Lilja[6,7], Kelly Hilven[8], Patrick Dupont[1,2], Koen Van Laere[2,5], Rik Vandenberghe[1,2,9]

[1]Laboratory for Cognitive Neurology, KU Leuven, Herestraat 49, 3000 Leuven, Belgium; [2]Alzheimer Research Centre KU Leuven, Leuven Institute of Neuroscience and Disease, Herestraat 49, 3000 Leuven, Belgium; [3]Department of Psychiatry, Oxford University, OX3 7JX Oxford, UK; [4]Old Age Psychiatry Department, University Hospitals Leuven, Herestraat 49, 3000 Leuven, Belgium; [5]Nuclear Medicine and Molecular Imaging Department, KU Leuven and University Hospitals Leuven, Herestraat 49, 3000 Leuven, Belgium; [6]GE Healthcare, Björkgatan 30, 753 23 Uppsala, Sweden; [7]Uppsala University, Department of Surgical Sciences, Radiology, Akademiska sjukhuset, 751 85 Uppsala, Sweden; [8]Laboratory for Neuroimmunology, KU Leuven, Herestraat 49, 3000 Leuven, Belgium; [9]Neurology Department, University Hospitals Leuven, Herestraat 49, 3000 Leuven, Belgium

Corresponding author: Rik Vandenberghe, Neurology Department, University Hospitals Leuven, Herestraat 49, 3000 Leuven, Belgium, phone: +32 (0)16 344280, fax: +32 (0)16 344285, e-mail: rik.vandenberghe@uz.kuleuven.ac.be

Keywords: amyloid PET, biomarker, Alzheimer's disease, preclinical AD.

Abstract

Purpose: Preclinical, or asymptomatic, Alzheimer's disease (AD) refers to the presence of positive AD biomarkers in the absence of cognitive deficits. This research concept is being applied to define target populations for clinical drug development. In a prospective community-recruited cohort of cognitively intact older adults, we compared two amyloid imaging markers within subjects: ^{18}F-flutemetamol and ^{11}C-Pittsburgh compound B (^{11}C-PIB).

Methods: In 32 community-recruited cognitively intact older adults aged between 65 and 80 years, we determined the concordance between binary classification based on ^{18}F-flutemetamol versus ^{11}C-PIB according to semiquantitative assessment (standardized uptake value ratio in composite cortical volume, $SUVR_{comp}$) and, alternatively, according to visual reads. We also determined the correlation between ^{18}F-flutemetamol and ^{11}C-PIB SUVR and evaluated how this was affected by the reference region chosen (cerebellar grey matter versus pons) and the use of partial volume correction (PVC) in this population.

Results: Binary classification based on semiquantitative assessment was concordant between ^{18}F-flutemetamol and ^{11}C-PIB in 94% of cases. Concordance of blinded binary visual reads between tracers was 84%. The Spearman correlation between ^{18}F-flutemetamol and ^{11}C-PIB $SUVR_{comp}$ with cerebellar grey matter as reference region, was 0.84, with a slope of 0.98. Correlations in neocortical regions were significantly lower with pons as reference region. PVC improved the correlation in striatum and medial temporal cortex.

Conclusions: For the definition of preclinical AD based on ^{18}F-flutemetamol, concordance with ^{11}C-PIB was highest using semiquantitative assessment with cerebellar grey matter as reference region.

1 Introduction

Biomarkers for Aβ accumulation in the brain play a central role in the National Institute on Ageing and Alzheimer's Association (NIA-AA) research definition of preclinical Alzheimer's disease (AD) [1]. Preclinical AD, also termed asymptomatic AD, refers to the presence of AD-related pathophysiological processes, such as amyloid aggregation, in individuals who do not have cognitive deficits [1, 2]. Cognitively intact individuals who are amyloid-positive are at increased risk for cognitive decline [3, 4]. Recent methods for defining amyloid-positivity include positron emission tomography (PET) amyloid imaging and $A\beta_{42}$ in cerebrospinal fluid assay. It is still largely unknown how the choice of a particular amyloid biomarker may affect the discrimination between amyloid-positive and amyloid-negative healthy subjects. This is important since an amyloid-positive status may define potential candidates for experimental (e.g. anti-amyloid) therapies in clinical drug development.

^{18}F-labeled tracers currently approved by the Food and Drugs Administration (FDA) and European Medicines Agency (EMA) for estimation of amyloid plaques in patients evaluated for cognitive decline are ^{18}F-flutemetamol [5, 6], ^{18}F-florbetaben [7], and ^{18}F-florbetapir [8]. The cortical retention of ^{18}F-flutemetamol has been compared to ^{11}C-Pittsburgh compound B (^{11}C-PIB) [9] in clinical populations such as amnestic mild cognitive impairment (aMCI) patients together with clinically probable AD patients [10], or aMCI and clinically probable AD together with healthy controls [11], but not in cohorts consisting exclusively of cognitively intact older adults. This is crucial since the discriminative value of a tracer may also depend on the population under study. The concordance between two tracers may be better in a mixed sample of patients and controls then in a group consisting exclusively of cognitively normal controls. In cognitively intact older adults ligand retention values may lie closer to threshold than in patients with probable AD and it has been hypothesized that ^{11}C-PIB could potentially outperform ^{18}F-labelled tracers under such conditions [12]. Other ^{18}F-labelled amyloid tracers (^{18}F-florbetaben [7], ^{18}F-florbetapir [8], ^{18}F-AZD4694 [13]) have also been compared with ^{11}C-PIB within subjects, again mostly in clinical patient populations combined with cognitively intact older adults [14, 15]. For these tracers, no direct comparisons have been performed in cohorts consisting exclusively of cognitively intact older adults. Cognitively intact older adults who are

amyloid-positive constitute the target population for a number of current clinical drug development programmes. The success of targeted molecular therapies may critically depend on the presence of the drug target. Accurate ascertainment of amyloid-positivity prior to inclusion may constitute one of the factors that determines the success of trials in preclinical AD (importance of high specificity), as well as the cost of screening for eligible subjects (importance of high sensitivity). Moreover, in cognitively intact older adults where amyloid levels are slightly to markedly elevated, the precise analysis method is essential. This may be less of an issue in patients with clinically probable AD who are well within the abnormal range. None of the studies comparing ^{18}F-flutemetamol and ^{11}C-PIB have evaluated the effect of reference region, magnetic resonance image (MRI) versus PET-based normalization or partial volume correction on the concordance between those tracers in cognitively normal older adults.

Therefore, the aim of this study was to directly compare ^{18}F-flutemetamol to ^{11}C-PIB within the same subjects in a prospective community-recruited cohort of cognitively intact older adults. We evaluated concordance between ^{18}F-flutemetamol versus ^{11}C-PIB binary classifications based on semiquantitative assessment and visual reads, as well as the correlations between the semiquantitative measures. We also estimated the impact of different image analysis methods on amyloid quantification.

2 Materials and methods

2.1 Participants

Thirty-two cognitively intact older controls (mean age 72 years, SD 5) participated in this study (Table 1). They were recruited through advertisement in local newspapers and through websites for seniors as part of a larger longitudinal study, asking for healthy volunteers between 65 and 80 years of age for participation in a scientific study at the University Hospital Leuven, Belgium, involving brain imaging. At screening, subjects underwent a detailed interview about medical history, a Mini Mental State Examination, a Clinical Dementia Rating, general physical and neurological examination, blood sampling, and a conventional neuropsychological assessment. Inclusion criteria were age between 65 and 80 years, MMSE $\geq$ 27, CDR = 0, and normal test scores on neuropsychological assessment. Inclusion was stratified for two genetic factors: BDNF

(*met* allele present or absent) and APOE (ε4 allele present or absent), as this cohort was part of a larger ^{18}F-flutemetamol study in healthy controls of the interactions between these polymorphisms [16, 17]. Exclusion criteria were neurological or psychiatric history and brain lesions on structural MRI. The protocol (EudraCT: 2009-014475-45) was approved by the Ethics Committee University Hospitals Leuven. Written informed consent was obtained from all subjects in accordance with the Declaration of Helsinki.

Table 1: Demographic and neuropsychological characteristics.

Gender (male/female)	21/11	
ApoE ε4	41%	
Age (years)	72 (4.5)	65-80
Education (years)	12.6 (3.2)	8-20
MMSE (/30)	29.1 (1.1)	27-30
AVLT TL (/75)	44.4 (7.1)	33-69
AVLT DR (/15)	8.8 (2.3)	5-13
AVLT %DR	78.5 (12.5)	55-100
BNT (/60)	54.3 (4.1)	41-60
AVF (# words)	24.6 (5.2)	16-40
LVF (# words)	35.0 (11.9)	14-61
RPM (/60)	35.5 (10.0)	15-54
TMT B/A	2.3 (0.6)	1.3-3.8

Second column: Mean (SD). Third column: Range. MMSE = Mini Mental State Examination; AVLT = Rey Auditory Verbal Learning Test; TL = total learning; DR = delayed recall; BNT = Boston Naming Test; AVF = Animal Verbal Fluency Test; LVF = Letter Verbal Fluency Test; RPM = Raven's Progressive Matrices; TMT = Trail Making Test part B divided by part A.

2.2 Amyloid PET

PET scans were acquired on a 16-slice Siemens Biograph PET/CT scanner (Siemens, Erlangen, Germany). Tracers were injected as a bolus in an antecubital vein (^{18}F-flutemetamol mean activity 150 MBq, SD 5 MBq, range 134-162 MBq; ^{11}C-PIB mean activity 363 MBq, SD 33

MBq, range 255-420 MBq). The ^{18}F-flutemetamol scan acquisition started 90 min after tracer injection and lasted for 30 min [6, 10, 16, 17]. The ^{11}C-PIB scan was obtained within 30 days from the ^{18}F-flutemetamol scan (mean 2 days, median 0 days, range -22 to 21 days). Three subjects could not come to the clinic within the 30 days period due to personal or health reasons and they received a ^{11}C-PIB scan within 32, 39, and 118 days from the ^{18}F-flutemetamol scan. Dynamic ^{11}C-PIB scan acquisition extended from 0 to 70 min post tracer injection. Prior to PET acquisition, a low-dose computed tomography scan of the head was performed for attenuation correction. Random and scatter correction were applied. The ^{18}F-flutemetamol measurement was rebinned into 6 frames of 5 min and the ^{11}C-PIB measurement between 40 and 70 min post injection was also rebinned into 6 frames of 5 min each. Images were reconstructed using Ordered Subsets Expectation Maximization (4 iterations x 16 subsets). A structural T1-weighted MRI was acquired on a 3T Philips Achieva scanner (3D turbo field echo sequence, 32-channel Philips SENSitivity Encoding head coil: coronal inversion recovery prepared 3D gradient-echo images, inversion time 900 ms, TE/TR 4.6/9.6, flip angle 8˚, voxel size 0.98 x 0.98 x 1.2 mm^3 [17]).

The ^{18}F-flutemetamol and the ^{11}C-PIB scans were preprocessed using Statistical Parametric Mapping 8 (SPM8, http://www.fil.ion.ucl.ac.uk/spm). The individual images of the 6 frames were realigned and summed for both data sets separately. The individual's ^{18}F-flutemetamol and ^{11}C-PIB PET summed images were co-registered to the subject's T1-weighted structural MRI. ^{18}F-flutemetamol and ^{11}C-PIB PET summed images were spatially normalized to the Montreal Neurological Institute (MNI) space using MRI. This was done in two steps. First, the MR image was spatially normalized to the SPM8 T1 template in MNI space using a unified segmentation approach. This generated the non-linear transformation parameters, as well as grey matter (GM), white matter (WM) and cerebrospinal fluid images. Next, these transformation parameters were applied to the individual's co-registered ^{18}F-flutemetamol and ^{11}C-PIB PET summed images to spatially normalize them to MNI space.

2.2.1 Semiquantitative analysis of amyloid PET

To measure specific tracer retention, standardised uptake value ratio (SUVR) images were calculated from the spatially normalized summed ^{18}F-flutemetamol images and from the spatially

normalized summed ^{11}C-PIB images (voxel size 2 x 2 x 2 mm^3) with the cerebellar GM used as reference region. The spatially standardised volumes of interest (VOIs) were identical for ^{18}F-flutemetamol and for ^{11}C-PIB image analysis. The cerebellar GM was defined based on the automated anatomical labelling (AAL) atlas (areas 91-108) and masked inclusively with subject-specific GM maps, with the threshold for masking set at > 0.3 [16, 17]. This reference region was used both for ^{18}F-flutemetamol and for ^{11}C-PIB images. As a secondary analysis, we also used pons as a reference region: this region was manually drawn on the SPM8 T1-template (13 axial slices of 2 mm) and then for each individual it was corrected to match the subject-specific anatomical boundaries of the pons based on the subject's spatially normalized MR image.

Our primary PET outcome measure was the mean SUVR in the composite cortical VOI ($SUVR_{comp}$) with cerebellar GM as reference region. The composite VOI consisted of 5 bilateral cortical areas [16, 17]. The spatially standardised VOIs were based on the AAL template. We also calculated mean SUVR in each of these regions separately and additionally in medial temporal (AAL 37-42), and occipital cortex (AAL 43-54), and striatum (AAL 71-74). The AAL VOIs were masked inclusively with subject-specific GM maps, with the threshold for masking set at > 0.3 [16, 17]. Mean SUVR was also estimated in subcortical WM (SWM), which was defined based on subject-specific WM maps thresholded at > 0.5.

The cut-offs for $SUVR_{comp}$ for binary classification were defined based on independent datasets re-analyzed using the MRI-based PET analysis method described above. The cut-offs were defined based on the statistical distance between the AD group and the HC as described in Vandenberghe et al. (2010), that is: ^{18}F-flutemetamol cut-off was estimated based on the Vandenberghe et al. (2010) dataset [10], and was equal to 1.38. The ^{11}C-PIB cut-off was calculated based on 37 clinically probable AD subjects and 23 age-matched healthy controls (datasets from Nelissen et al. (2007) [18], Vandenberghe et al. 2010 [10], and Ahmad et al. 2014 [19]) and was equal to 1.22. Note that the used 1.38 ^{18}F-flutemetamol cut-off is lower than the cut-off defined by Vandenberghe et al. (2010) or Thurfjell et al. (2014) for a purely PET-based approach, probably due to exclusion of more white matter signal by the current MRI-based method in the amyloid-negative cases. We also verified our binary case classification using the purely PET-based method with narrow VOIs and SUVR cut-offs with reference to cerebellar GM

as used by Thurfjell et al. (2014). For this method, the cut-off with the neuropathological modified Consortium to Establish a Registry for Alzheimer's Disease score as standard-of-truth was 1.57 [20].

As a further secondary analysis, we performed a semiquantitative analysis based on partial volume corrected (PVC) data. PVC was based on the MRI using the modified Müller-Gärtner method [16, 17, 21].

2.2.2 Visual reads

^{18}F-flutemetamol and ^{11}C-PIB scans were visually evaluated by 3 independent readers blinded to all subject information: two certified nuclear medicine physicians (reader 1 K.V.L, reader 2 K.G.) and a certified psychiatrist (reader 3 M.V.), experienced in reading amyloid scans. All readers had successfully completed the GE Healthcare electronic reader training program for ^{18}F-flutemetamol images. The visual read was done on summed orthogonal PET images in native space, scaled to the image maximum intensity value and displayed with a modifiable rainbow (NIH) colour scale. Each reader received an individually randomized list of ^{18}F-flutemetamol and ^{11}C-PIB images which were evaluated in separate sessions. Readers were asked to assign scans as positive or negative and to rate their overall confidence in classifying the image on a scale from 1 to 5 (5 being the highest confidence). The final assignment was based on a majority verdict.

2.3 Statistical analysis

The primary analyses were intended to evaluate in cognitively intact older adults:

1. The concordance between binary classification based on ^{18}F-flutemetamol versus ^{11}C-PIB according to semiquantitative $SUVR_{comp}$ assessment.
2. The concordance of binary visual reads of ^{18}F-flutemetamol versus ^{11}C-PIB.
3. The correlation between ^{18}F-flutemetamol and ^{11}C-PIB $SUVR_{comp.}$ Normality of data distribution was tested using the Shapiro-Wilk test. Correlations were evaluated using (a) Spearman rank correlation coefficients ρ if distributions deviated from normality, and (b) using slopes of linear regression m. The agreement between ^{18}F-flutemetamol and ^{11}C-PIB $SUVR_{comp}$ was tested by a Bland-Altman analysis [22].

The secondary analyses evaluated in cognitively intact older adults:

1. The agreement between readers of the visual classification. This was analysed by means of Fleiss' Kappa (κ).
2. Readers' confidence in visual binary classification of the PET scans. This was analysed by three-factor repeated measures ANOVA, with reader (3 levels: reader 1 vs 2 vs 3) and tracer (2 levels: ^{18}F-flutemetamol vs ^{11}C-PIB) as within-subject factors, and concordance of binary visual reads (2 levels: concordant vs discordant) as between-subject factor.
3. The correlation between ^{18}F-flutemetamol and ^{11}C-PIB SUVR in a set of 9 separate regions.
4. The correlation between ^{18}F-flutemetamol and ^{11}C-PIB SUVR values using the pons as reference region.
5. The correlation between PVC-corrected ^{18}F-flutemetamol and PVC-corrected ^{11}C-PIB SUVR values.

Statistical analyses were performed in Statistica 11 (http://www.statsoft.com/) and Matlab R2013b (http://www.mathworks.com).

3 Results

Regional and composite SUVR values of ^{18}F-flutemetamol (W = 0.68-0.86, $P < 0.002$) and ^{11}C-PIB (W = 0.69-0.87, $P < 0.006$) were not normally distributed. Therefore in the subsequent analyses we used Spearman ρ coefficient.

Binary classification based on semiquantitative cut-offs was concordant between ^{18}F-flutemetamol versus ^{11}C-PIB in 94% of the cases (Figure 1a). Based on ^{18}F-flutemetamol $SUVR_{comp}$ 5 out of 32 subjects (16%) were assigned to the amyloid-positive category (Figure 1a, Figure 2). Based on ^{11}C-PIB $SUVR_{comp}$, 7 out of 32 subjects (22%) were assigned to the amyloid-positive category (Figure 1a, Figure 2). Two cases were discordant between ^{18}F-flutemetamol and ^{11}C-PIB (cases 8 and 31, Figure 1a, Figure 2). These subjects were assigned to the amyloid-negative category based on ^{18}F-flutemetamol and to the amyloid-positive category based on ^{11}C-PIB.

Concordance of binary visual reads between tracers was 84% (Figure 1b). Based on ^{18}F-flutemetamol scans 3 out of 32 subjects (9%) were assigned to the amyloid-positive category (Figure 1b, Figure 2). According to ^{11}C-PIB scans, 6 out of 32 subjects (19%) were assigned to

the amyloid-positive category (Figure 1b, Figure 2). Out of 5 discordant cases, one subject was read as positive for ^{18}F-flutemetamol but negative for ^{11}C-PIB (case 24, Figure 1b, Figure 2, Figure 3), and 4 were read as positive for ^{11}C-PIB but negative for ^{18}F-flutemetamol (cases 17, 19, 29, 31, Figure 1b, Figure 2). Fleiss κ for inter-reader agreement was 0.86 for ^{18}F-flutemetamol, and 0.93 for ^{11}C-PIB.

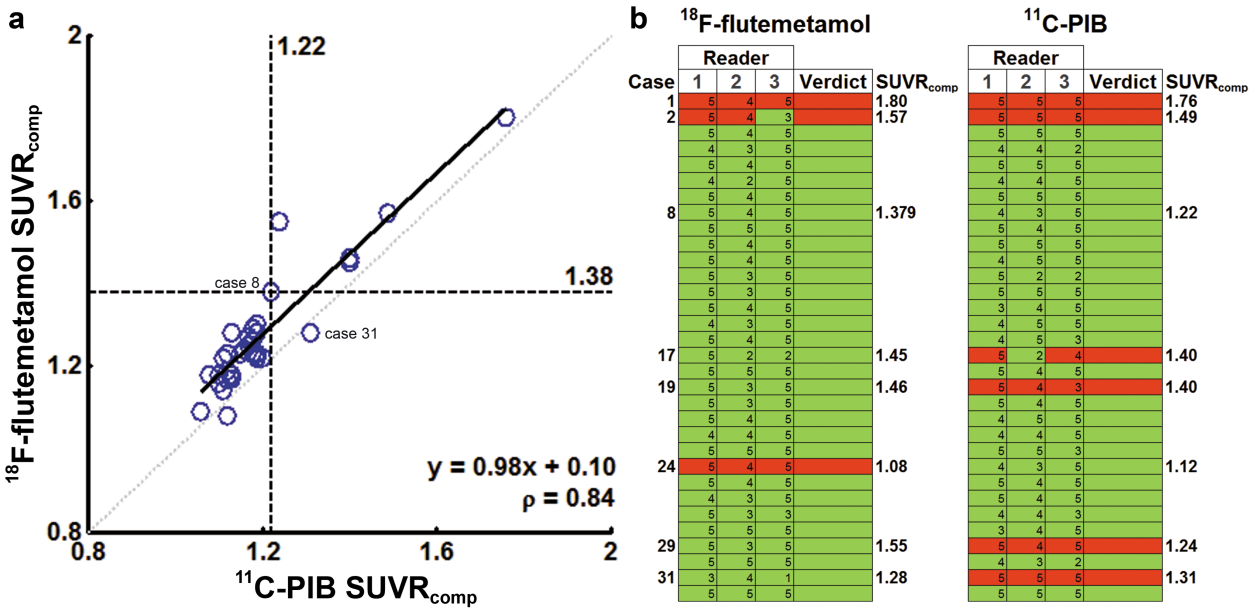

Figure 1: Concordance between binary semiquantitative (a) and visual (b) classifications of ^{18}F-flutemetamol and ^{11}C-PIB scans. (a) Dashed lines = SUVR cut-offs. (b) Red = positive scan; green = negative scan. Values in red and green cells = confidence levels of the readers.

When we analysed readers' confidence in visual classification of ^{18}F-flutemetamol and ^{11}C-PIB scans we found a significant main effect of reader ($F_{2,60}$ = 12.3, P = 0.00003): reader 1 (r1) and 3 (r3) were more confident than reader 2 (r2) (r1 > r2 P = 0.0001, r3 > r2 P = 0.0006) (Figure 4a). We also found a significant main effect of concordance of visual classification: readers were more confident when classifying concordant cases compared with discordant cases ($F_{1,30}$ = 5.1, P = 0.03) (Figure 4b). No other effects were found.

^{18}F-flutemetamol and ^{11}C-PIB SUVR values were highly correlated in the composite cortical VOI, in all neocortical VOIs and in subcortical white matter (Table 2; Figure 5). The correlations in striatum and medial temporal cortex were weaker (Table 2; Figure 5). The slopes

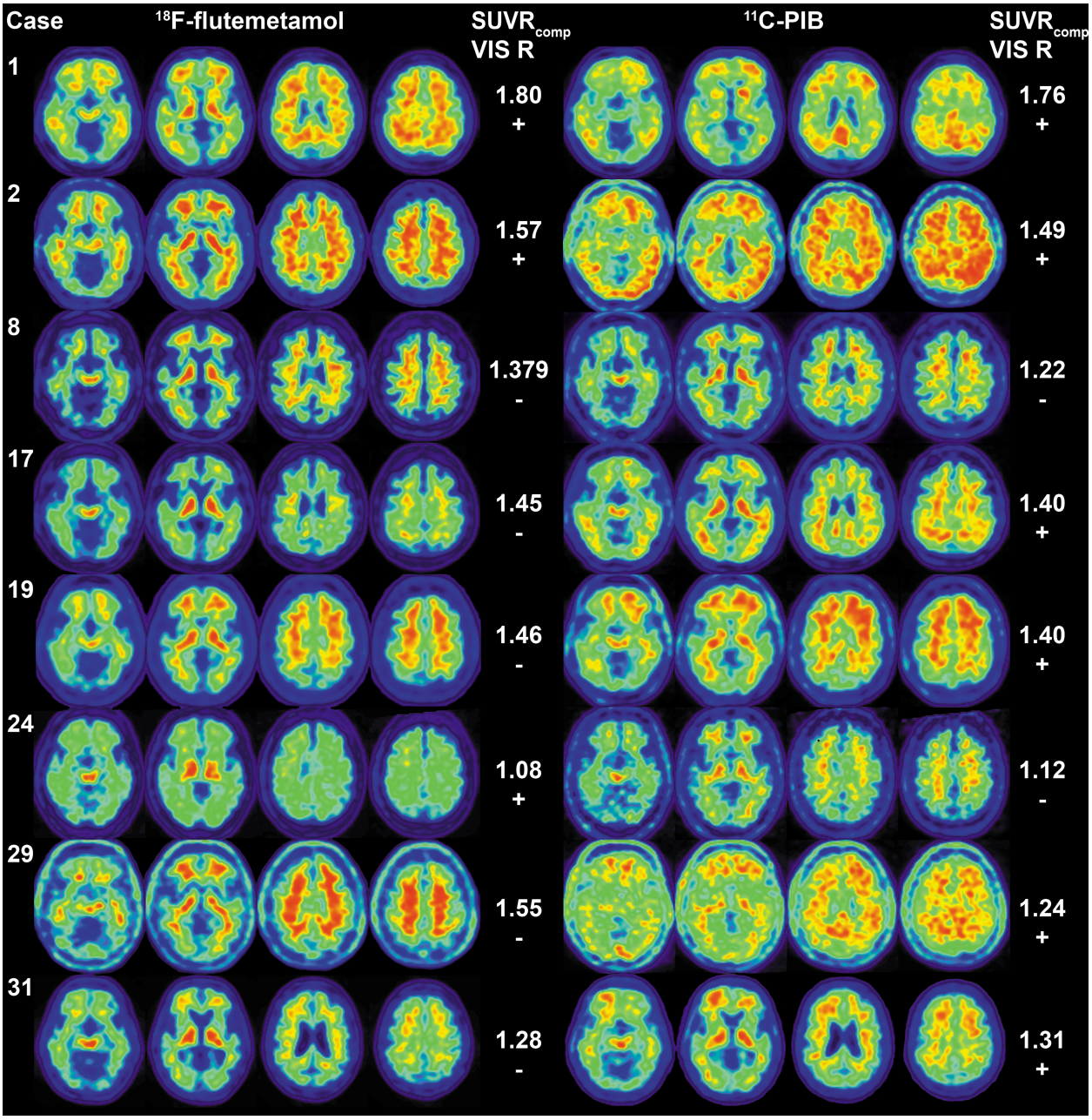

Figure 2: Representative summed PET images of the discordant cases between ^{18}F-flutemetamol and ^{11}C-PIB scans based on semiquantitative and visual classification. For the sake of comparison we also displayed two positive cases who were concordantly classified by semiquantitative and visual approach. Brain sections show axial slices at -4, 10, 24, 38 MNI *z* coordinates. On the right side of the brain sections $SUVR_{comp}$ values (at the top) and results of visual reads (VIS R, at the bottom, + positive scan, - negative scan) are shown. Images are scaled to a maximum intensity in an image.

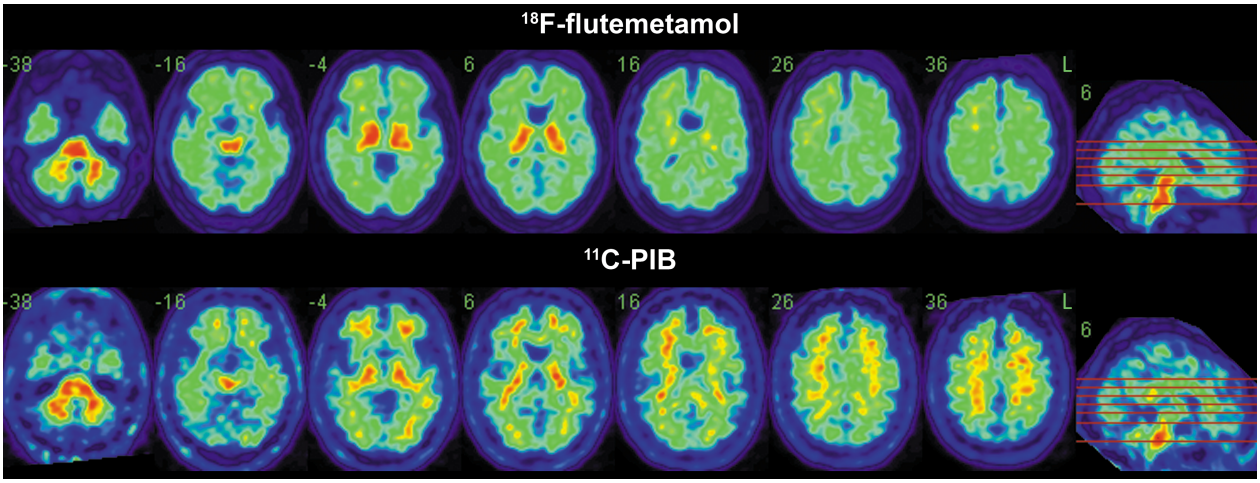

Figure 3: Detailed view on case 24. Left upper corners show MNI coordinates. Right upper corners show brain orientation. Images are scaled to a maximum intensity in an image.

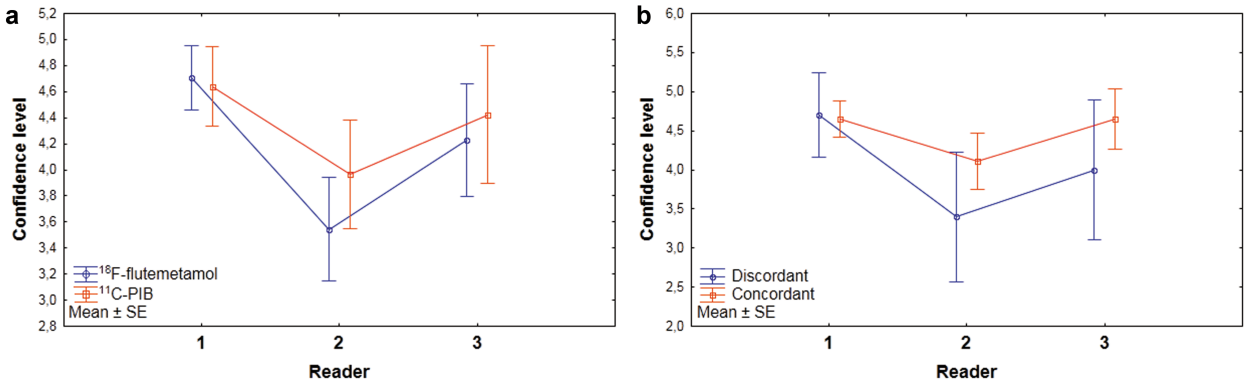

Figure 4: Analysis of readers' confidence in visual binary classification of ^{18}F-flutemetamol and ^{11}C-PIB scans. Main effect of reader (a). Main effect of concordantly versus discordantly classified cases (b).

of linear regression were close to 1 in all neocortical regions and subcortical white matter (Table 2; Figure 5). Slopes in striatum and medial temporal cortex were lower (Table 2; Figure 5). The Bland-Altman analysis [22] showed a good agreement between ^{18}F-flutemetamol and ^{11}C-PIB $SUVR_{comp}$, with a systematic bias towards higher ^{18}F-flutemetamol SUVR values (Figure 6).

When we applied the Thurfjell et al. (2014) PET-based processing method and autopsy derived SUVR cut-off with reference to cerebellar GM, 4 out of 32 ^{18}F-flutemetamol scans (13%) were classified as amyloid-positive. In three cases, the MRI-informed and the purely PET-based processing methods yielded discordant classification: two subjects were classified as amyloid-negative based on the PET-based method and as amyloid-positive based on the MRI-informed

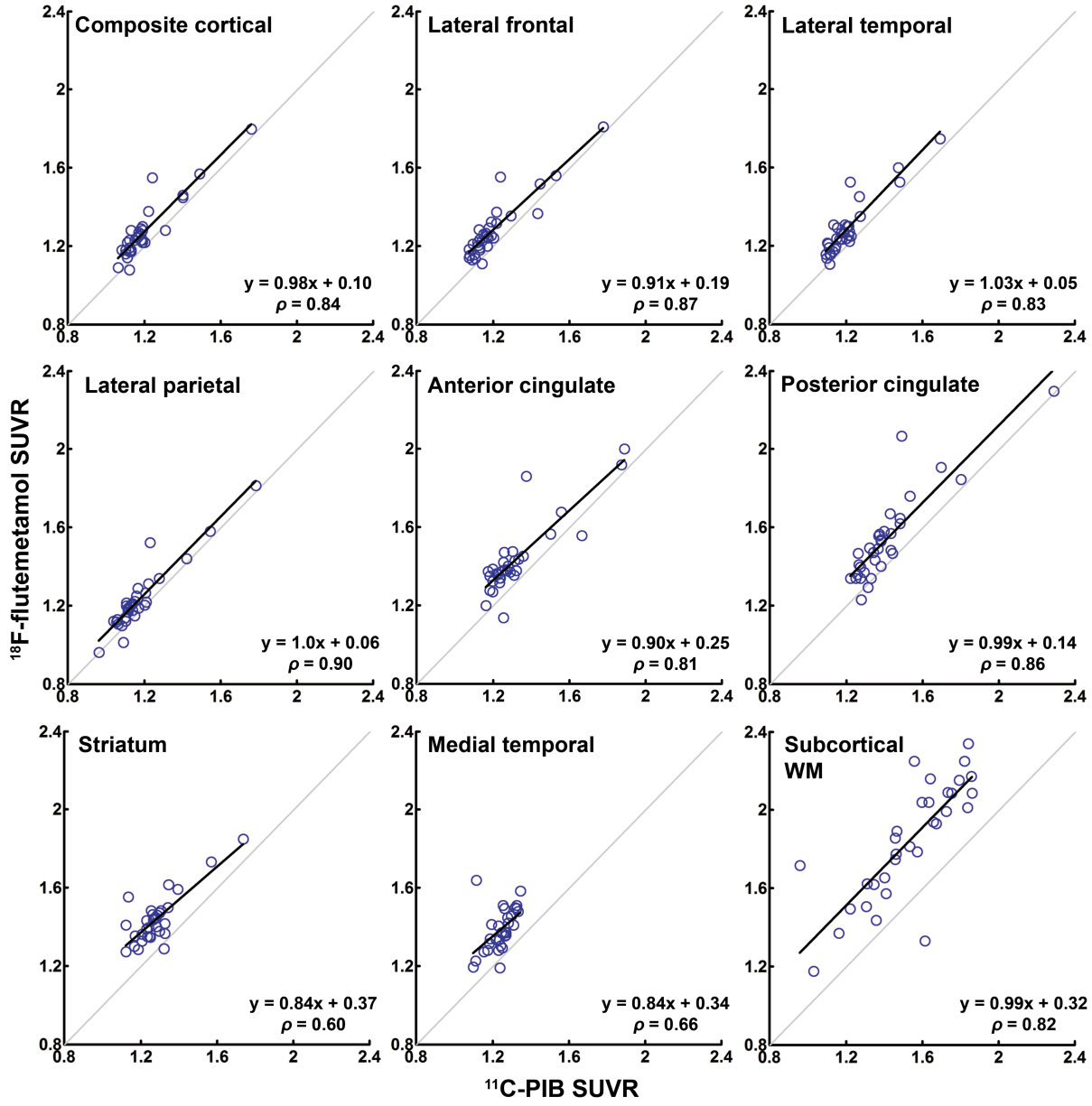

Figure 5: Regional correlations between ^{18}F-flutemetamol and ^{11}C-PIB SUVRs. WM = white matter.

method (case 19 and 29, Figure 1b, Figure 2, $SUVR_{comp}$ based on purely PET-based processing method 1.45 and 1.47 respectively), one subject showed the inverse pattern (case 31, Figure 1b, Figure 2, $SUVR_{comp}$ based on purely PET-based processing method 1.61). The correlation between ^{18}F-flutemetamol and ^{11}C-PIB scans analysed by the purely PET-based processing method was high in composite cortical VOI and in all neocortical VOIs (Table 2).

When pons was used as reference region, the correlation between ^{18}F-flutemetamol and

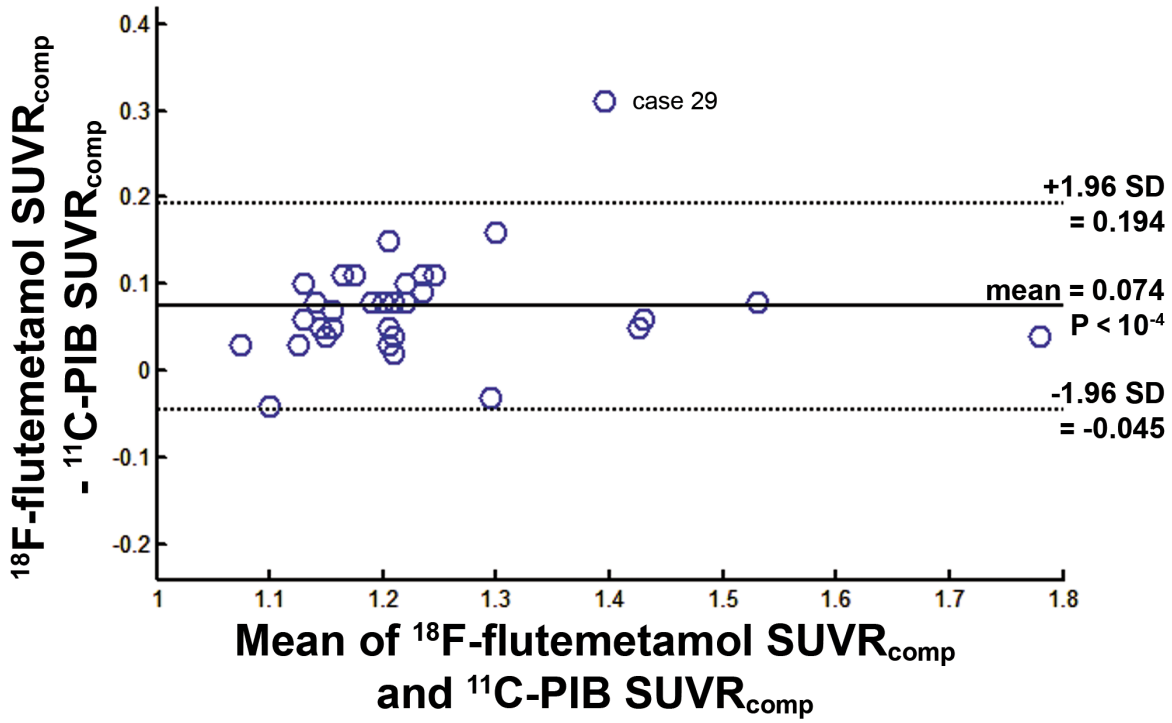

Figure 6: Agreement between ^{18}F-flutemetamol and ^{11}C-PIB SUVRs based on Bland-Altman analysis.

^{11}C-PIB SUVRs was weaker in the composite cortical VOI and in neocortical VOIs. This difference was statistically significant in the lateral parietal VOI (P = 0.007) (Table 2). The correlation however was stronger in striatum, medial temporal cortex, and subcortical WM when pons was used as reference region than when cerebellar GM was used. This difference was statistically significant in subcortical WM (P = 0.004) (Table 2). With pons as reference region, the slopes of linear regression were close to 0.5 and were significantly less steep than with cerebellar GM as reference region in all VOIs (P < 0.0001) except for subcortical WM where slope was 0.9 (Table 2).

PVC did not significantly alter ρ and slopes for the correlation between ^{18}F-flutemetamol and ^{11}C-PIB SUVR values in the composite cortical VOI or any of the neocortical VOIs (Table 2). In striatum, medial temporal cortex and subcortical WM, PVC improved ρ or slope significantly (Table 2).

Table 2: Region-wise correlations between ^{18}F-flutemetamol and ^{11}C-PIB SUVRs for different analysis methods

	MRI-informed method						PET-based method	
	Cerebell GM		Pons		Cerebell GM & PVC		Cerebell GM	
Region	*m*	*ρ*	*m*	*ρ*	*m*	*ρ*	*m*	*P*
Composite cortical	0.98	0.84	**0.49**	0.69	0.96	0.90	**0.72**	0.86
Lateral frontal	0.91	0.87	**0.49**	0.76	0.91	0.89	**0.72**	0.85
Lateral temporal	1.03	0.83	**0.47**	0.70	1.03	0.87	**0.73**	0.75
Lateral parietal	1.00	0.90	**0.50**	**0.63**	0.97	0.92	**0.74**	0.92
Anterior cingulate	0.90	0.81	**0.54**	0.79	0.89	0.90	**0.73**	0.82
Posterior cingulate	0.99	0.86	**0.56**	0.78	0.98	0.83	**0.72**	0.92
Lateral occipital	1.03	0.77	**0.43**	0.72	0.94	0.86	**0.67**	0.84
Striatum	0.84	0.60	**0.52**	0.81	**0.95**	**0.87**	-	-
Medial temporal	0.84	0.66	**0.53**	0.79	**0.99**	0.68	**0.76**	0.70
Subcortical WM	0.99	0.82	0.90	**0.96**	0.98	**0.95**	-	-

Cerebell GM = cerebellar grey matter; WM = white matter; PVC = partial volume correction; *m* = slope of linear regression; *ρ* = Spearman correlation coefficient. All correlations reached $P \leq 0.0001$, except for the correlation in striatum with cerebellar GM as reference region $P = 0.0003$. Bold font shows significant differences at $P < 0.05$ for comparison of *m* and *ρ* with columns 2-3, respectively. Not corrected for multiple comparisons.

4 Discussion

To our knowledge this is the first study comparing ^{18}F-flutemetamol to ^{11}C-PIB in a cohort consisting exclusively of cognitively intact older adults, without patients with cognitive deficits. Our results provide evidence for a close correspondence between the two amyloid tracers even at this preclinical stage.

We detected a few more amyloid-positive cases with ^{11}C-PIB scan (7 out of 32) than with ^{18}F-flutemetamol scan (5 out of 32). This differs from previous comparisons that included only AD and MCI [10] or AD, MCI, together with HC [11], where concordance between ^{18}F-flutemetamol and ^{11}C-PIB was 100%. In the Hatashita et al. study [11] the cut-offs for

semiquantitative assessment were not defined independently from the test sample and this may also have contributed to this complete concordance. In our study the cut-offs were based on independent datasets.

The values in the discordant cases in our study were around the cut-off, except for case 24 (see below). Near-threshold values may render the binary division between amyloid-positive and -negative cases in cognitively normal individuals more difficult. Amyloid accumulation is a progressive process and the amyloid-positive cases are distributed over range of continuous values rather than bimodally. Hence, among cognitively normal controls a binary classification into positive and negative subjects is somewhat artificial. Individuals with the intermediate amyloid levels may either remain at this level or may be heading towards further pathological amyloid aggregation [23]. Subjects around the cut-off may be accumulating amyloid at a higher rate than those subjects who are further removed from the cut-off [23] and in this sense may be of special interest for potentially disease-modifying drug trials. To investigate the prevalence and the meaning of these cases with sufficient power a joint longitudinal approach including different centres would be necessary. In such an approach a standardized quantification of amyloid deposition, such as centiloid scale [24], would facilitate the comparison. Values close to threshold probably explain the higher rate of discordance in visual reads in our study compared to what has been found in AD and MCI [10, 11]. We however met one exception: in case 24, ^{18}F-flutemetamol SUVR was far removed from the cut-off and nevertheless the ^{18}F-flutemetamol scan was read as positive by all 3 readers with relatively high confidence. When evaluating this scan in retrospect, the outcome of the read may have been determined by the fact that tracer retention was similarly low in white matter and in neocortex. As a consequence, the pattern of gyral indentation was lost and the cortical surface relatively even. This was not true for the ^{11}C-PIB scan. The similarity in ^{18}F-flutemetamol retention between neocortex and white matter and the even appearance of the surface may have led to the positive read despite the low neocortical SUVR. This underscores the usefulness of semiquantitative measures when evaluating normal control ^{18}F-flutemetamol scans. The overall confidence of readers in visual evaluation of scans was high, however, the confidence of all readers was lower when evaluating discordant cases compared with concordant cases. This indicated that a subset of scans in this population is

particularly difficult to read.

As a further difference with previous comparative studies [10], the correlation between ^{18}F-flutemetamol and ^{11}C-PIB SUVR values in subcortical white matter (Table 2) was higher than previously observed (in [10] r = 0.36). The definition of the white matter VOI may have been more accurate in the current study as it was based on the MRI. A white matter VOI that is defined based on PET may be affected by spill-over between grey and white matter and this may differ between ^{18}F-flutemetamol and ^{11}C-PIB, yielding lower correlations in previous studies [10].

We also evaluated how differences in the analysis method affected the concordance and the correlation with ^{11}C-PIB. PVC did not substantially alter correlations between ^{18}F-flutemetamol and ^{11}C-PIB in neocortical VOIs, but affected the correlation in striatum and medial temporal cortex in a positive sense. The latter area is known to be particularly susceptible to partial volume effects. Second, using pons as a reference region resulted in substantially lower correlations between ^{18}F-flutemetamol and ^{11}C-PIB in neocortical regions (Table 2). Only in striatum, medial temporal cortex, and subcortical WM did pons as a reference region yield better correlations (Table 2). Finally, the correlations of SUVRs were the same when ^{18}F-flutemetamol and ^{11}C-PIB scans were analysed with a purely PET-based method [20] compared to our MRI-based method [16] (Table 2). It however is worth noting that the slopes for the correlations between ^{18}F-flutemetamol and ^{11}C-PIB were substantially lower for the purely PET-based method than when MRI was used to independently define the regions to be used for analysis of the two PET modalities.

Practical implications

The FDA and EMA approvals of amyloid imaging are for visual reads and are restricted to patients with cognitive decline. For research use in cognitively intact individuals, our findings suggest that semiquantitative assessment would be preferable above visual reads. In cognitively intact older individuals cerebellar grey matter would be the preferred reference region compared with pons. PVC would be advantageous for evaluation of medial temporal cortex and subcortical regions. Concordance between ^{18}F-flutemetamol and ^{11}C-PIB was better when regions were based on MRI rather than for PET-based regions.

Conclusion

Our study of amyloid markers in asymptomatic older adults provides evidence that semiquantitative measures of ^{18}F-flutemetamol with cerebellar grey matter as a reference are closely similar to what one would obtain if ^{11}C-PIB was used, in particular if MRI is used to define the regions of interest. Concordance for visual reads tended to be less convincing in this population.

5 Acknowledgements

We would like to thank the staff of Nuclear Medicine, Neurology, and Radiology at the University Hospitals Leuven. Special thanks to Carine Schildermans, Dorien Timmers, Kwinten Porters, and Mieke Steukers, for help with the study. Financial support was provided by the Foundation for Alzheimer Research SAO-FRMA (09013, 11020, 13007); Research Foundation Flanders (G.0660.09); KU Leuven (OT/08/056, OT/12/097); IWT VIND; IWT TGO BioAdapt AD; Belspo IAP (P7/11); Research Foundation Flanders senior clinical investigator grant to R.V. and K.V.L.; Research Foundation Flanders doctoral fellowship to K.A; and KH is supported by the Research Fund KU Leuven (OT/11/087 and CREA/14/023). ^{18}F-flutemetamol was provided by GE Healthcare free of charge for this academic investigator-driven trial.

Compliance with Ethical Standards

Funding: This study was funded by the Foundation for Alzheimer Research SAO-FRMA (grant numbers 09013, 11020, 13007); Research Foundation Flanders (grant number G.0660.09); KU Leuven (grant numbers OT/08/056, OT/12/097); IWT VIND; IWT TGO BioAdapt AD; Belspo IAP (grant number P7/11); Research Foundation Flanders senior clinical investigator grant to R.V. and K.V.L.; Research Foundation Flanders doctoral fellowship to K.A; and KH is supported by the Research Fund KU Leuven (grant numbers OT/11/087 and CREA/14/023). ^{18}F-flutemetamol was provided by GE Healthcare free of charge for this academic investigator-driven trial.

Conflict of Interest: Katarzyna Adamczuk declares that she has no conflict of interest. Jolien Schaeverbeke declares that she has no conflict of interest. Natalie Nelissen declares that she has no conflict of interest. Veerle Neyens declares that she has no conflict of interest. Mathieu Vandenbulcke declares that he has no conflict of interest. Karolien Goffin declares that she has no conflict of interest. Johan Lilja declares that he has no conflict of interest. Kelly Hilven declares that she has no conflict of interest. Patrick Dupont declares that he has no conflict of interest. Koen Van Laere declares that he has no conflict of interest. Rik Vandenberghe was the PI of the phase 1 and 2 ^{18}F-flutemetamol trials. UZ Leuven has had a clinical trial agreement for these trials with GEHC. RV has a consultancy agreement with GEHC. ^{18}F-flutemetamol was provided by GEHC for the conduct of reported investigator-driven trial free of cost.

Ethical approval: All procedures performed in studies involving human participants were in accordance with the ethical standards of the institutional and/or national research committee and with the 1964 Helsinki declaration and its later amendments or comparable ethical standards.

Informed consent: Informed consent was obtained from all individual participants included in the study.

References

1. Sperling RA, Aisen PS, Beckett LA, Bennett DA, Craft S, Fagan AM, et al. Toward defining the preclinical stages of Alzheimer's disease: recommendations from the National Institute on Aging-Alzheimer's Association workgroups on diagnostic guidelines for Alzheimer's disease. Alzheimers Dement. 2011;73:280-292.
2. Dubois B, Feldman HH, Jacova C, Cummings JL, Dekosky ST, Barberger-Gateau P, et al. Revising the definition of Alzheimer's disease: a new lexicon. Lancet Neurol. 2010;911:1118–1127.
3. Knopman DS, Jack JC, Wiste HJ, Weigand SD, Vemuri P, Lowe V, et al. Short-term clinical outcomes for stages of NIA-AA preclinical Alzheimer disease. Neurology. 2012;7820:1576–1582.
4. Vos SJ, Xiong C, Visser PJ, Jasielec MS, Hassenstab J, Grant EA, et al. Preclinical Alzheimer's disease and its outcome: a longitudinal cohort study. Lancet Neurol. 2013;1210:957–965.
5. Koole M, Lewis DM, Buckley C, Nelissen N, Vandenbulcke M, Brooks DJ, et al. Whole-body biodistribution and radiation dosimetry of 18F-GE067: a radioligand for in vivo brain amyloid imaging. J Nucl Med. 2009;505:818–822.
6. Nelissen N, Van Laere K, Thurfjell L, Owenius R, Vandenbulcke M, Koole M, et al. Phase 1 study of the Pittsburgh compound B derivative 18F-flutemetamol in healthy volunteers and patients with probable Alzheimer disease. J Nucl Med 2009;508:1251– 1259.
7. Rowe CC, Ackerman U, Browne W, Mulligan R, Pike KL, O'Keefe G, et al. Imaging of amyloid beta in Alzheimer's disease with 18F-BAY94-9172, a novel PET tracer: proof of mechanism. Lancet Neurol. 2008;72:129–135.
8. Wong DF, Rosenberg PB, Zhou Y, Kumar A, Raymont V, Ravert HT, et al. In vivo imaging of amyloid deposition in Alzheimer disease using the radioligand 18F-AV-45 (florbetapir F18). J Nucl Med. 2010;516:913–920.
9. Klunk WE, Engler H, Nordberg A, Wang Y, Blomqvist G, Holt DP, et al. Imaging brain amyloid in Alzheimer's disease with Pittsburgh Compound-B. Ann Neurol. 2004;553:306–319.
10. Vandenberghe R, Van Laere K, Ivanoiu A, Salmon E, Bastin C, Triau E, et al. 18F- flutemetamol amyloid imaging in Alzheimer disease and mild cognitive impairment: a phase 2 trial. Ann Neurol. 2010;683:319–329.
11. Hatashita S, Yamasaki H, Suzuki Y, Tanaka K, Wakebe D, Hayakawa H. [18F]Flutemetamol amyloid-beta PET imaging compared with [11C]PIB across the spectrum of Alzheimer's disease. Eur J Nucl Med Mol Imaging. 2014;412:290–300.
12. Jagust WJ. Amyloid imaging: coming to a PET scanner near you. Ann Neurol 2010;683:277-278.
13. Cselényi Z, Jönhagen ME, Forsberg A, Halldin C, Julin P, Schou M, et al. Clinical validation of 18F-AZD4694, an amyloid-β-specific PET radioligand. J Nucl Med. 2012;533:415–424.
14. Vandenberghe R, Adamczuk K, Dupont P, Van Laere K, Chételat G. Amyloid PET in clinical practice: Its place in the multidimensional space of Alzheimer's disease. Neuroimage Clin. 2013;26:497–511.
15. Rowe CC, Pejoska S, Mulligan RS, Jones G, Chan JG, Svensson S, et al. Head-to-head comparison of 11C-PiB and 18F-AZD4694 (NAV4694) for β-amyloid imaging in aging and dementia. J Nucl Med. 2013;546:880–886.
16. Adamczuk K, De Weer AS, Nelissen N, Chen K, Sleegers K, Bettens K, et al. Polymor- phism of Brain Derived Neurotrophic Factor influences β amyloid load in cognitively intact Apolipoprotein E ε4 carriers. Neuroimage Clin. 2013;2:512–520.
17. Adamczuk K, De Weer AS, Nelissen N, Dupont P, Sunaert S, Bettens K, et al. Functional changes in the language network in response to increased amyloid deposition in cognitively intact older adults. Cereb Cortex. 2014;bhu286.
18. Nelissen N, Vandenbulcke M, Fannes K, Verbruggen A, Peeters R, Dupont P, et al. Abeta amyloid deposition in the language system and how the brain responds. Brain. 2007;130:2055–2069.
19. Ahmad R, Goffin K, Van den Stock J, De Winter FL, Cleeren E, Bormans G, et al. In vivo type 1 cannabinoid receptor availability in Alzheimer's disease. Eur Neuropsychopharmacol. 2014;242:242–250.
20. Thurfjell L, Lilja J, Lundqvist R, Buckley C, Smith A, Vandenberghe R, et al. Automated Quantification of 18F-Flutemetamol PET Activity for Categorizing Scans as Negative or Positive

for Brain Amyloid: Concordance with Visual Image Reads. J Nucl Med. 2014;55:1623-1628.
21. Müller-Gärtner HW, Links JM, Prince JL, Bryan RN, McVeigh E, Leal JP, et al. Measurement of radiotracer concentration in brain gray matter using positron emission tomography: MRI-based correction for partial volume effects. J Cereb Blood Flow Metab. 1992;124:571–583.
22. Bland JM, Altman DG. Statistical methods for assessing agreement between two methods of clinical measurement. Lancet. 1986;18476:307–310.
23. Villemagne VL, Burnham S, Bourgeat P, Brown B, Ellis KA, Salvado O, et al. Amyloid β deposition, neurodegeneration, and cognitive decline in sporadic Alzheimer's disease: a prospective cohort study. Lancet Neurol. 2013,12:357-67.
24. Klunk WE, Koeppe RA, Price JC, Benzinger TL, Devous MD Sr, Jagust WJ, et al. The Centiloid Project: standardizing quantitative amyloid plaque estimation by PET. Alzheimers Dement. 2015,11:1-15.